International Journal of Geosciences, 2023, 14, 655-676
https://www.scirp.org/journal/ijg
ISSN Online: 2156-8367
ISSN Print: 2156-8359

Assessment of the Spectral Decomposition Techniques in the Evaluation of Hydrocarbon Potential of "BOMS" Field, Coastal Swamp Niger Delta, Nigeria

Charles Chibueze Ugbor, Onyebuchi Samuel Onyeabor*

Department of Geology, University of Nigeria, Nsukka, Nigeria
Email: *onyebuchionyeabor@gmail.com

How to cite this paper: Ugbor, C.C. and Onyeabor, O.S. (2023) Assessment of the Spectral Decomposition Techniques in the Evaluation of Hydrocarbon Potential of "BOMS" Field, Coastal Swamp Niger Delta, Nigeria. *International Journal of Geosciences*, **14**, 655-676.
https://doi.org/10.4236/ijg.2023.147035

Received: May 4, 2023
Accepted: July 28, 2023
Published: July 31, 2023

Abstract

This study employs the different approaches of the spectral decomposition techniques to evaluate the hydrocarbon potential of the reservoir and analyse to determine the most efficient spectral decomposition technique with better resolution using the "BOMS" Field, coastal swamp depobelt Niger Delta, Nigeria. A good number of drilled wells have failed both in the Niger Delta Basin and other basins due to a poor understanding of the reservoir properties in advance of drilling and identifying the best approach will help to minimize this risk. Seismic and well logs data together with the Hampson Russel 10.3 software were used for the study. The target reservoirs were identified from the suite of well logs at the horizons with low gamma ray, high resistivity, and low acoustic impedance between TVD (ft) of 10,350 - 10,450 ft. The analysis of the amplitude spectrum of the seismic data revealed that the distortion of interest lies between 5 - 60 Hz. Seismic data were then spectrally decomposed into several frequencies such as low frequency (15 Hz), mid-frequency (31 Hz), and high frequency (46 Hz) where distortions were observed. Time-frequency slices of 15 Hz and 23 Hz provided clearer events (potential hydrocarbon sand) indicated by high amplitude envelope (2200 - 2400) and amplitude anomalies. While the amplitude dropped in the mid-frequency (31 Hz), the high amplitude envelope and the high energy completely disappeared in the high (46 Hz) time-frequency slice. A comparison of the Short-time Fourier transform and the Basic Pursuit algorithm revealed that the Basic Pursuit provided a better resolution of the reservoir characteristics than the former. The Red, Green and Blue (RGB) colour blending model indicated that the channel was consistent with the low-frequency section and amplitude anomaly.

Keywords

Amplitude, Hydrocarbon Evaluation, Spectral Analysis, Reservoir Sand, Basic Pursuit, Convolution

1. Introduction

The superposition of several frequencies makes up the frequency of seismic traces (S. Sun, 2006; Castagna *et al*., 2006). To further analyze the seismic data to obtain minute details, there is a need to extract these several frequencies. There are several proposed and published methods for this in literature; These include Short Time window Fourier Transform (STFT), Wavelet Transform [1] [2] S-Transform (ST) ([3], and Matching Pursuit Decomposition (MPD) [4]). Seismic amplitudes of traces in the stack section are a total of individual amplitudes which are recorded at different angles of incidence [5]. Changes in these constituent amplitudes have been utilized in the industry as good indicators of fluid types and lithology [6]. As a result of this, many equations and approximations have been proposed and utilized to monitor the amplitude changes and also used as a tool for both lithological discrimination and the detection of hydrocarbons.

Seismic attributes are made up of some basic information derived from the seismic data: frequency, time, amplitude, and attenuation. Usually, many seismic attributes being used are derived from post-stack seismic data which is obtained from the stacked and migrated seismic data volume. Horizon attributes are picked along the tracked horizon or time-slice. Time-derived attributes are used to acquire structural details. Frequency-derived and amplitude-derived attributes are used to study the reservoir and stratigraphic properties of the reservoir. Amplitude attributes are known to be very robust and useful, but integrating frequency attributes has helped in discovering additional geologic layering [7]. With this adopted use of seismic attribute technology, much attention has been brought to the use of both frequency attributes with amplitude attributes. One of the most used frequency attributes with huge popularity in the industry is spectral decomposition.

Spectral decomposition is known to be a distinctive innovative seismic attribute mainly used for reservoir imaging and as a hydrocarbon indicator developed and commercialized originally by BP, Apache Corp. and Landmark [8]. This method requires creating a suite of amplitude maps using a sequence of seismic frequency slices across the area of interest, these maps are then integrated to obtain a better image resolution of the target, interval thickness and lithologic heterogeneities instead of traditional broad-band seismic displays. We can observe that in the last decade, many published works explained the possible implementation of this new approach to separate both vertical and lateral lithologies and pore-fluid changes. It also explained how it could be used to identify minute frequency changes and delineate the stratigraphic traps associated with hydrocarbons [9]. Further research has been done on the tuning effect on spectral characteristics. Some of these studies have been published in a series of companion papers by [10] [11] [12] and [13]; the studies stated that the tuning effect in thin-layer is significant and depends on both the ratio of the layer thickness over wavelength as well as offset. However, dispersion/attenuation will further alter the spectral characteristics that are obtained from tuning and this tuning effect alone cannot cause the brightening of the AVO anomalies. Therefore, the spectral variations observed are a resultant effect of both the tuning of the seismic waves in porous sands and attenuation/dispersion.

Spectral decomposition analysis also functions as a direct hydrocarbon Indicator. Direct hydrocarbon indicator technique using bright spot analysis entails identifying high amplitude anomalous areas in the seismic section in comparison with others [14]. This is the first practical evidence which helped to identify the existence of fluid in the "Bright spots" which was noted especially for gas identification in early 1970. But with future drilling activities showed that other geologic cases exhibit this same amplitude response type according to Reference [15], other than hydrocarbons which will most likely result in a wrong bright spot and lead to a dry hole if drilled.

Reference [16] used well logs and 3D seismic to evaluate the hydrocarbon trapping potential and 3D structural analysis of subsurface structures of Otu Field, Niger Delta with the aid of the log data, a network of faults, horizon delineation, and extraction of the RMS amplitude which shows that field contains hydrocarbon economically.

Reference [17], predicted the reservoir system quality at Kwe Field Niger Delta and identified its depositional environment using the petrophysical properties of the reservoir and well-log data. He identified 7 reservoirs in the Kwe field.

Reference [18] in order to identify new prospects evaluated the Olive field in Niger Delta using well logs, check shots and 3D seismic data. He established the time and depth structural maps, porosity ranging from 24.63% - 34.01%, hydrocarbon saturation ranging from 70.93% - 78.86% with seismic interpretation showing the field to be well faulted and seismic amplitude attribute maps characterized by high amplitude range (bright spot) in the zone surrounded by the structural traps and hence the identification of Four hydrocarbon prospects in the field.

Reference [19] used well-log analysis and some petrophysical properties like water saturation, porosity, permeability, bulk water, Net to gross, and hydrocarbon saturation to estimate the hydrocarbon prospect of the site and identified 4 sand reservoirs.

Although they are different ways to perform the decomposition of the spectra, all the decomposition methods aim to extract the constant frequency sections or cubes. Once these constant frequency sections are computed, the user can investigate and analyze the frequency expressions of the targeted zone or formation. The latter expressions might be used to infer the fluid presence, lithology changes, or thickness estimations [20].

Reference [21] made use of matching-pursuit decomposition for instantaneous spectral analysis in detecting low-frequency shadows beneath hydrocarbon reservoirs. A case history of using spectral decomposition and coherency to interpret incised valleys is shown by [22]. Reference [8] made use of windowed spectral analysis to derive discrete-frequency energy cubes for applications in reservoir characterization. Reference [23] proved that an average frequency attribute derived from sine curve-fitting in a particular area correlates with shale volume.

In this study, Spectral decomposition was carried out using 3D Prestack seismic data from the BOMS oilfield in the southeastern Niger Delta to analyze the reflector surface and to investigate the seismic amplitude anomalies if it is associated with hydrocarbon or not. Furthermore, the appraisal of the Fourier and Basic Pursuit transforms as a spectral decomposition technique in the evaluation of hydrocarbon potential using BOMS Field, coastal swamp depobelt Niger Delta, Nigeria to evaluate the hydrocarbon potential of the reservoir and analyse to determine the most efficient spectral decomposition technique.

2. Geology of the Study Area

The Niger Delta Basin is known as an extensional rift basin which is found in the Gulf of Guinea and projects throughout Niger Delta Province (**Figure 1**). It lies on the passive continental margin which is near the western coast of Nigeria. The delta has southwestward progradation from the Eocene to the Present, which formed many of the depo-belts representing the main active part of the delta at every development stage [24]. The sediment's mean thickness is approximately 10 km at the centre of the depo-belts and the volume of the sediment is estimated as 500,000 km^3 [25]. The Province of Niger Delta has one identified petroleum system. [26] [27] noted this as the Akata-Agbada Petroleum System (Tertiary Niger Delta). Reference [28] further researched and also concurred with one petroleum system within the Niger Delta, formed during the southern Atlantic opening at the triple junction which started during the Late Jurassic and continued to the Cretaceous. Based on Reference [26], the delta began to develop in the Eocene with sediment accumulation which now has a thickness of about 10 km. The area is made up of a sedimentary basin geologically which has three Formations: Benin Formations, Agbada, and Akata. The Akata Formation comprises shale which is formed during the marine transgressive cycle and is the major source rock in this basin [28]. Agbada Formation is predominantly made of sand deposited in a paralic environment [29].

This makes up the oil and gas reservoir that is within the basin [30]. Agbada Formation is referred to by [31] as a zone of transition with intercalation of shale and sand. The Agbada Formation has hydrocarbon traps which mostly occur as rollover anticlines in growth faults (dip closures) and some stratigraphic traps.

The faults are mostly listric and also form major barriers leading to accumulated hydrocarbon compartmentalization. Benin Formation stratigraphically covers the upper part of the Delta and lies above Agbada Formation. It consists of unconsolidated sands approximately 2000 m thick [32]. It is made up of coastal plain sands as it is deposited in a fluvial environment [33] (See **Figure 2**).

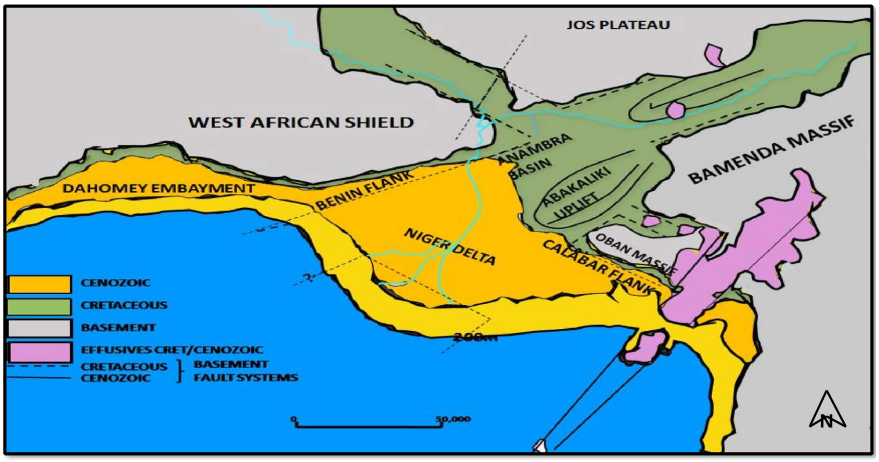

Figure 1. Geologic map of the *Niger Delta* (redrawn from [34]).

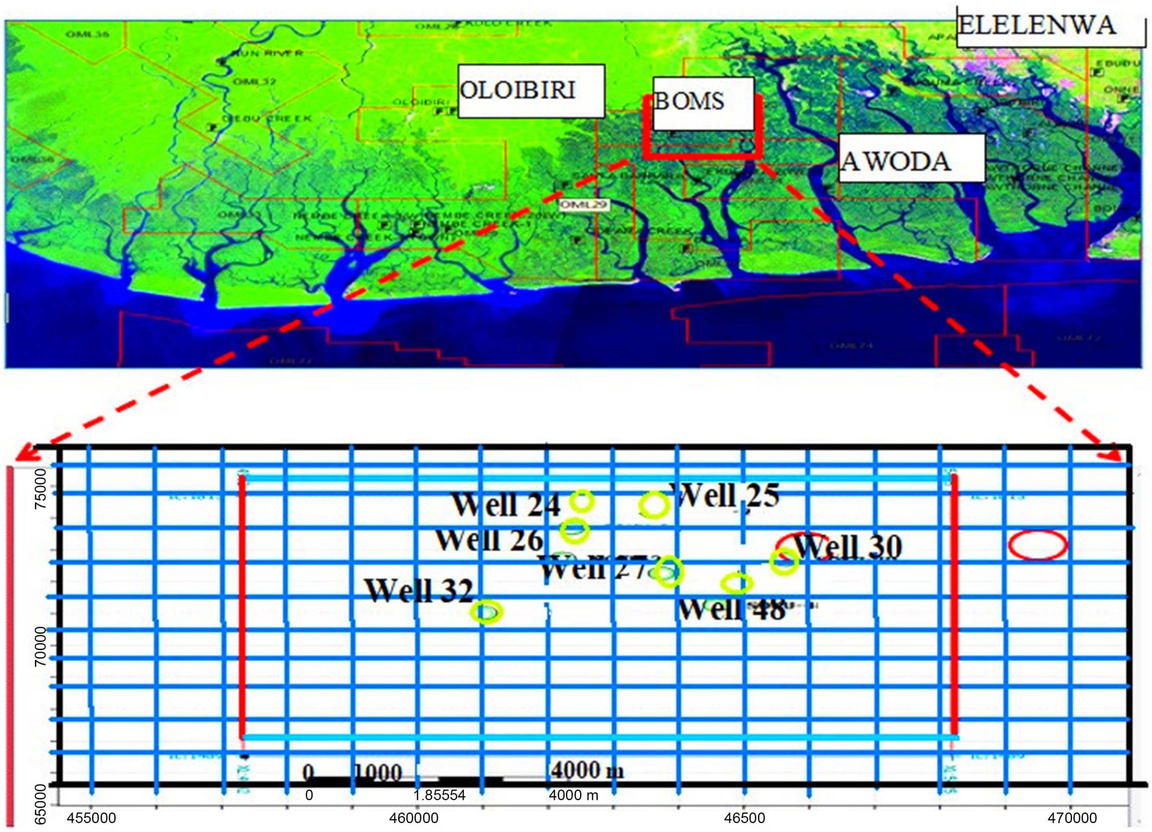

Figure 2. Map of *BOMS* field location in *Niger Delta* and base map of the study area with seven wells as plotted by the author during the course of this study.

3. Materials and Method of Study

3.1. Materials

The data used in this work are well logs data from BOMS field in the coastal swamp depobelt within the Niger Delta basin obtained from SPDC Port Harcourt. These data were analyzed using Hampson Russell Software (HRS). This includes the 3D pre stack time migrated seismic volumes and suite of well log profiles (gamma ray, caliper, Resistivity, density, and P-wave).

Two wells (Well 26 and 30) have a full suite of wireline logs over the reservoir interval. Well 26 is shown in Figure 3. It, is located in the Southwest of the field has a total depth of 11,661 ft and Well 30 is shown in Figure 4. It is situated at South east of the field totals 12,000 ft with full suite of wireline logs. The well information is summarized in Table 1. Of these two wells, gamma ray log is consistent with the sand shale sequence of the Niger Delta as the resistivity log reflects its characteristics at the regions of sand and shale sequences. Other wells some were with no compressional waves were excluded from the analysis.

Suite of well logs is principally analyzed when describing zones of interest depending on the character of gamma ray and Resistivity logs. In this, delineation of target zones becomes paramount to estimate the thickness or potentiality of a Formation. To achieve this, we have color coded gamma ray log with two colors: yellow reflects decrease in gamma ray equivalent to sand cutoff less than 75 API and brown color reflects increase in gamma ray that reflects shale zone cutoff less than 75 API. However, within the reservoir sand (65 ft and 83 ft in both wells), we notice intercalations of sand and little shale but above the reservoir, shale thickness is seen greater across both wells which probably act as cap rocks as shown in Figure 5 and Figure 6.

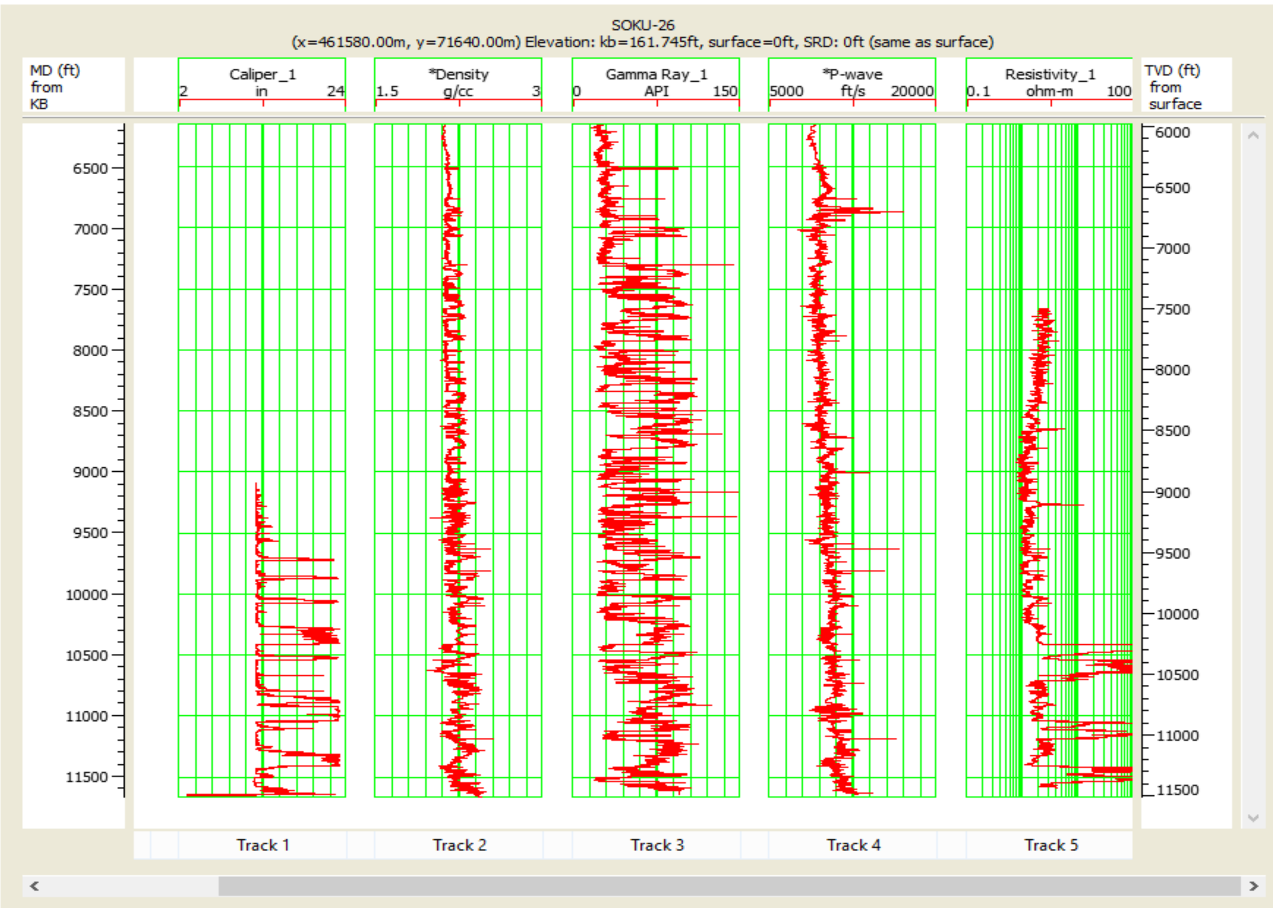

Figure 3. Suite of wireline logs for Well 26 showing density log, caliper log, gamma ray log, resistivity log and sonic log.

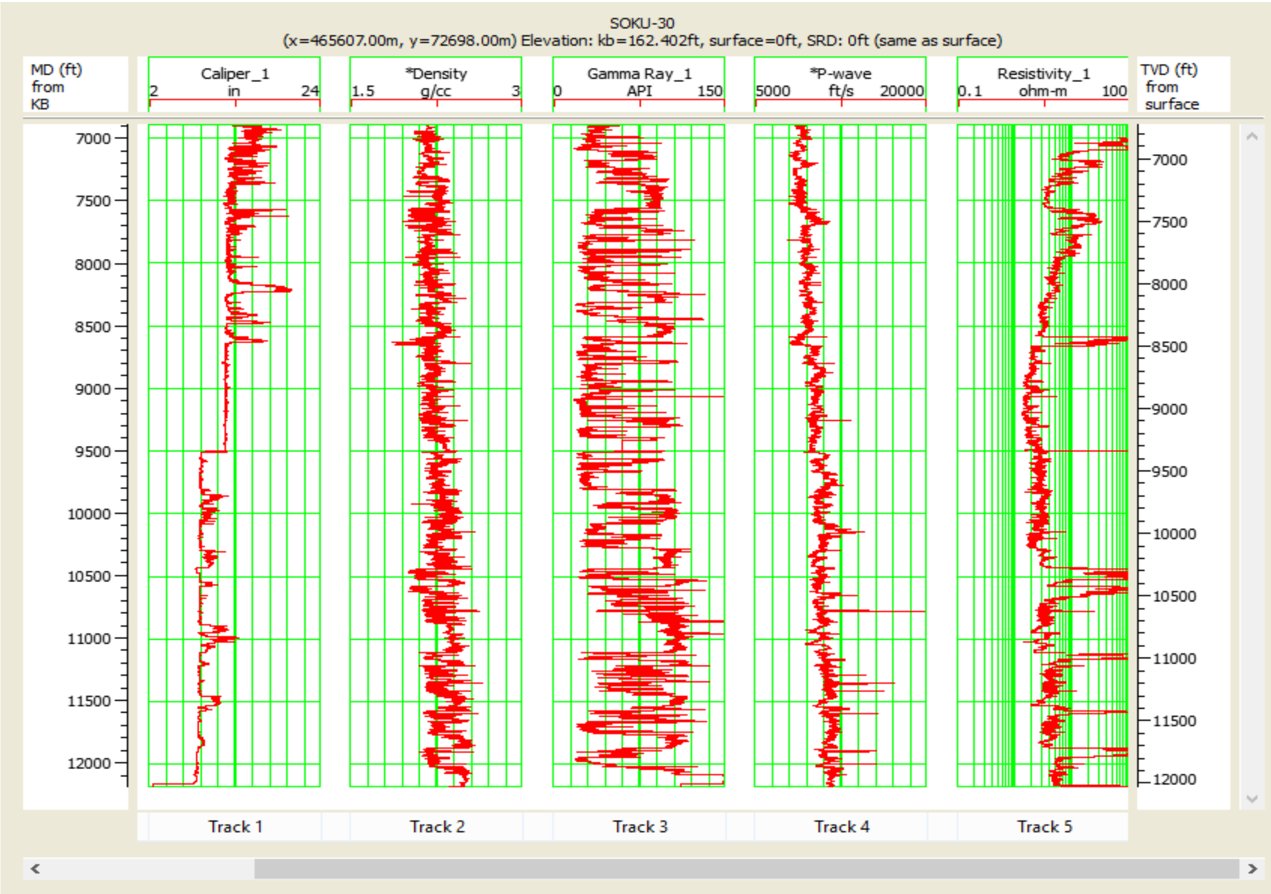

Figure 4. Suite of wireline logs for *Well* 30 showing density log, caliper log, gamma ray log, resistivity log and sonic log.

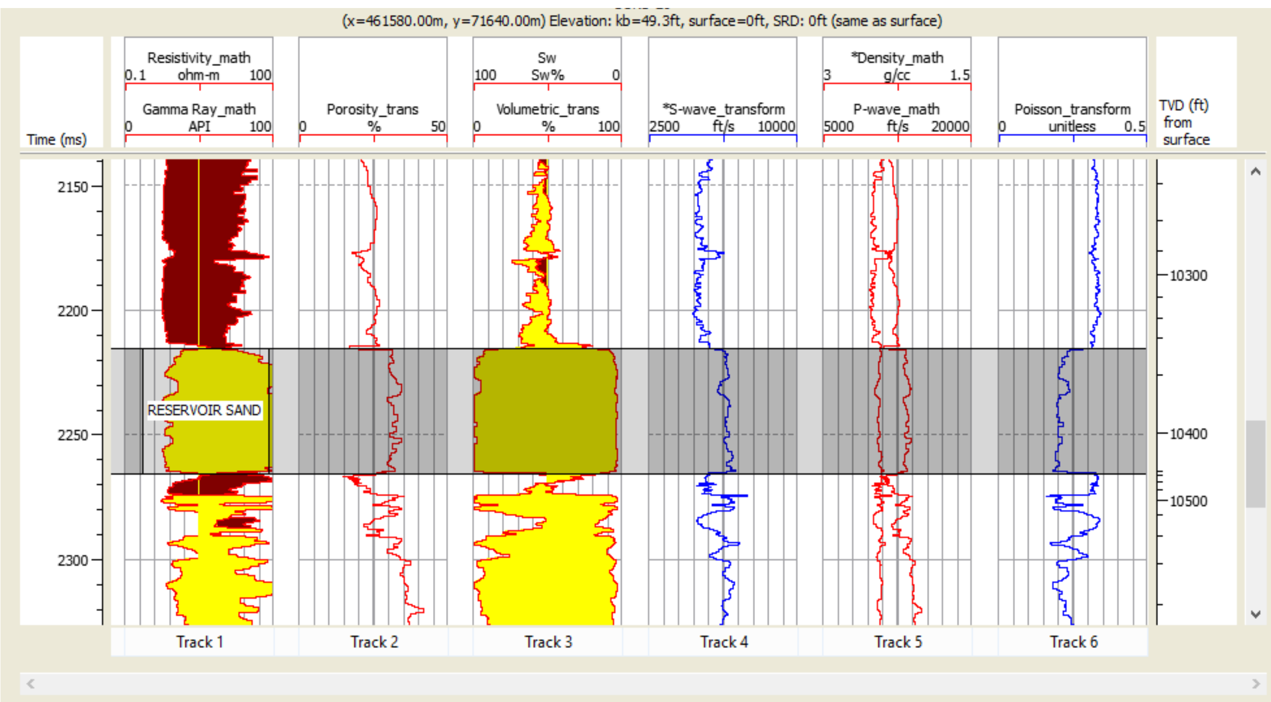

Figure 5. Reservoir sand delineation at *BOMS* 26.

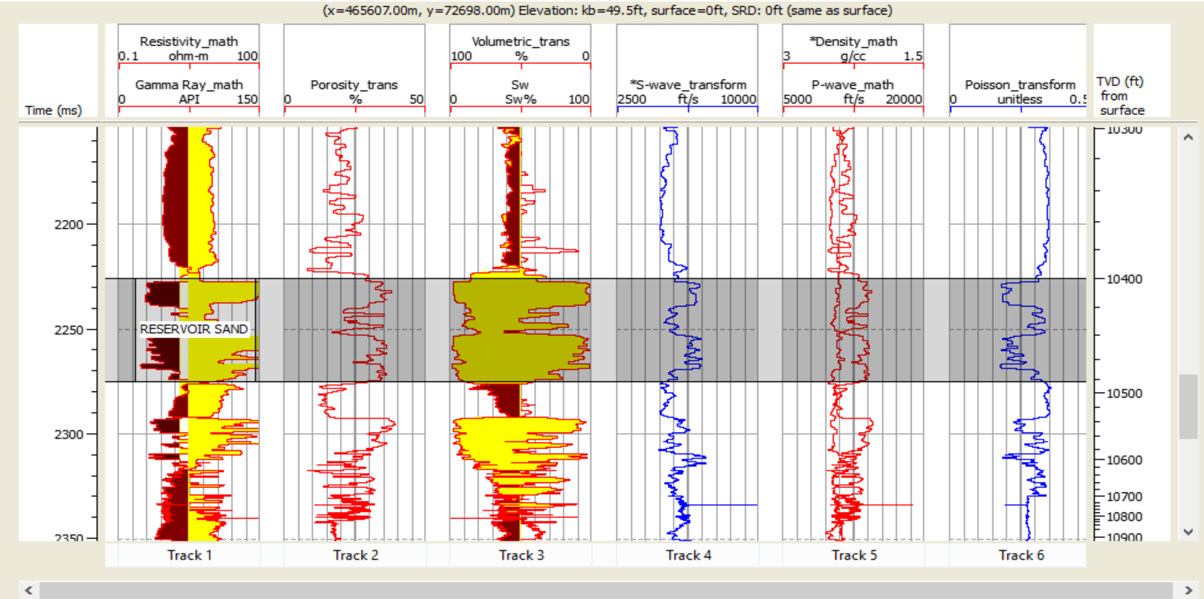

Figure 6. Reservoir sand delineation at *BOMS* 30.

Table 1. Seven wells employed for the study with their respective suite of wireline logs available and total depth penetrated for each well.

WELL	Gamma Ray (API)	Caliper (in)	Resistivity (ohm)	Density (g/cc)	P-wave (ft/s)	S-wave (ft/s)	Total Depth (ft)
WELL 24	Yes	Yes	Yes	Yes	Yes	No	9500
WELL 25	Yes	Yes	Yes	Yes	Yes	No	*11,000
WELL 26	Yes	Yes	Yes	Yes	Yes	No	11,661
WELL 27	Yes	Yes	Yes	Yes	No	No	12,406
WELL 30	Yes	Yes	Yes	Yes	Yes	No	12,197
WELL 32	Yes	Yes	Yes	Yes	No	No	12,200
WELL 48	Yes	Yes	Yes	Yes	No	No	10,459

The seismic data was also quality-checked for consistency and high integrity. A high resolution amplitude anomaly is shown in Figure 7 and the range of frequency covered is shown in Figure 8.

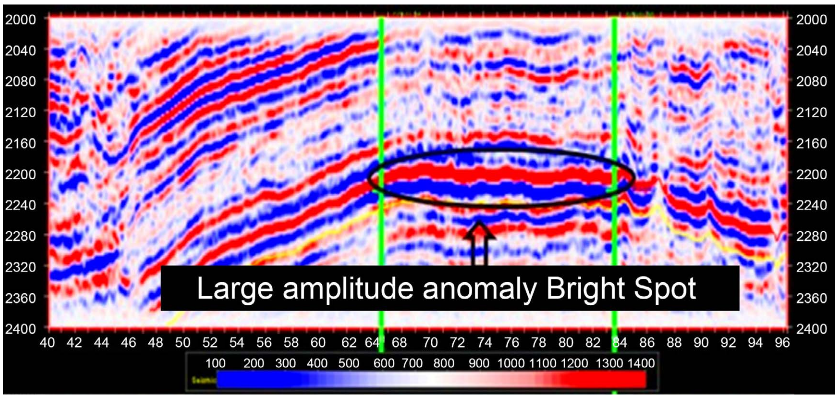

Figure 7. Colored seismic data showing two wells (*Well* 26, *Well* 30) within the interval of 2000 ms to 2400 ms. Probable gas channel (black eclipse) is observed within the HORIZON A AND HORIZON B.

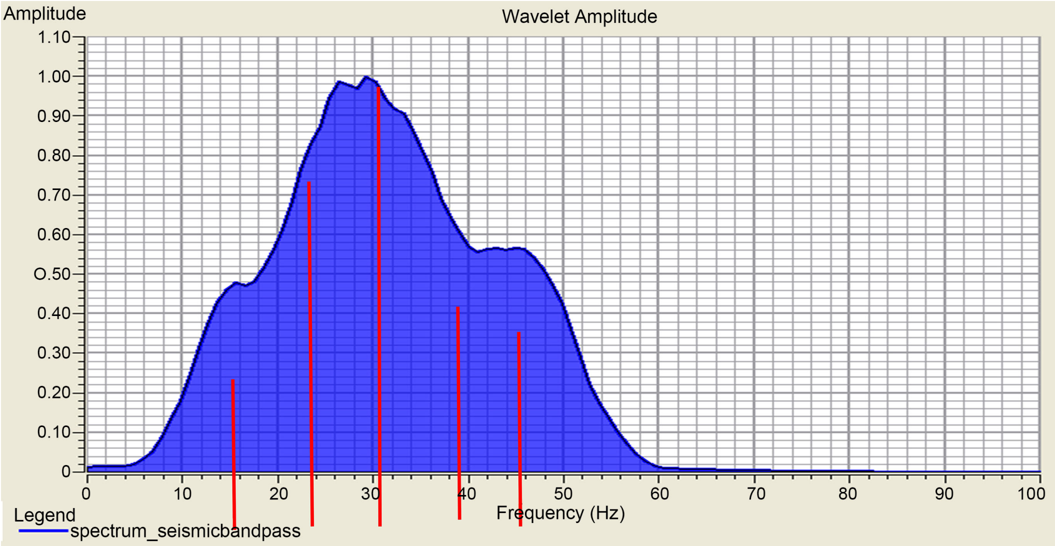

Figure 8. Frequency Spectrum displaying the highest time frequency resolution of the seismic data taken within 200 - 2400 ms. It ranges from 5 HZ - 60 HZ. The data will be spectrally decomposed to these ranges of frequencies: 15 HZ (low frequency), 23 HZ, 31 HZ (mid frequency), 39 HZ and 46 Hz (high frequency).

3.2. Method of Study

The study was carried out by running a set of analyses using the well and seismic data. These included,

1) Create time slices of the input seismic data to observe any subtle anomalies in amplitude around the zone of interest.

2) Create the AMPLITUDE SPECTRUM of the seismic data to know the frequency ranges of the data.

3) Create the amplitude slices of the STFT outputs using raw amplitude and RMS options for interpretation.

4) Comparison between Short Time Fourier Transform and Basic Pursuit algorithm.

5) Sorting of the frequencies for RGB blending.

3.3. Selection of Reservoir Interval and Wells

Well-log suites are basically analyzed to describe zones of interest depending on the behavior of Resistivity logs and gamma rays. In this, the delineation of target zones becomes paramount to estimating the thickness or potentiality of a Formation. To get this, a gamma-ray log was colour-coded with two colours: yellow reflecting a decline in gamma-ray equivalent to sand (cutoff <65 API) and a brown colour reflecting an increase in gamma-ray which indicates shale zone (cutoff >65). In addition, within the sand reservoir (95 ft and 126 ft in both wells), sand intercalations and a small amount of shale but on top of the reservoir were very evident, shale thickness is larger across the wells which possibly functions as cap rocks.

AMPLITUDE SPECTRUM

Spectrum analysis was done using Hampson Russell. From the frequency spectrum of the seismic data, three main peaks were identified within the frequency range of 5 Hz and 60 Hz. Therefore in this analysis, seismic data was decomposed using three main frequencies, that is, 15 Hz (low frequency), 23 Hz, (mid frequency), and 46 Hz (High frequency) to assess the response of the potential reservoir or target zone. It is readily seen that frequency responses are changing from one frequency component to another. "This can be related to the characteristic frequencies of the Formations which are controlled by their physical properties (lithology and thickness) and fluid content" and a hydrocarbon indicator [35] (**Figure 9**).

The short time Fourier transform algorithm was carried out on the seismic data of the inline range (1489 - 1819) and x-line range (4992 - 5425) within 2000 - 2400 ms. However, the seismic data has a large amplitude anomaly around the time 2200 ms suspected to be a gas sand-related anomaly. In this seismic section, we see a very strong amplitude anomaly in the southeastern part, which could indicate shallow gas sand with a high amplitude anomaly on the amplitude map. The channel feature is clearly shown in the red color key (3800 - 4698) around the wells.

4. Result and Discussion

4.1. Short Fourier Transform

Prior to applying the spectral decomposition, we need to identify the frequency spectrum of the seismic data. **Figure 8** shows the frequency spectrum of the seismic data, where we found the peaks indicated in the frequency of 5 Hz and 60 Hz respectively. Therefore in this analysis, the seismic data was decomposed using five frequencies, that is, 15 Hz (low frequency), 23 Hz, 31 Hz (mid frequency), 39 Hz and 46 Hz (High frequency) to assess the response of the potential reservoir or target zone. The short time Fourier transform algorithm has

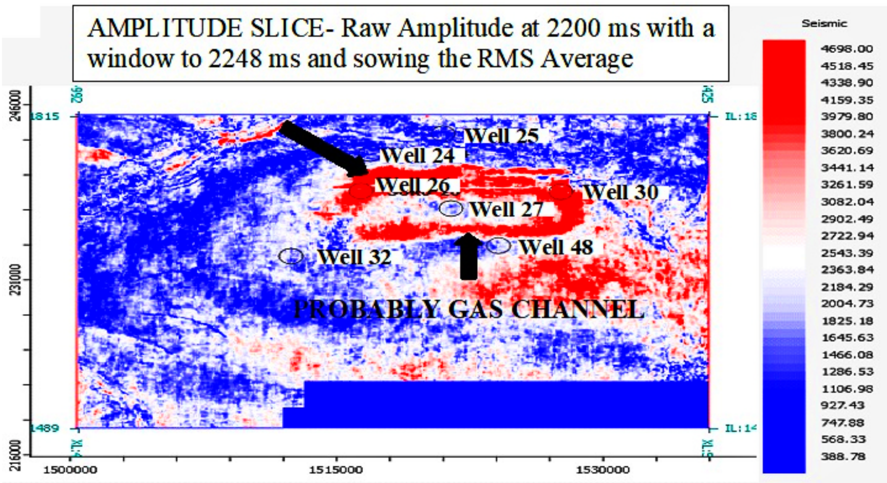

Figure 9. Time slice (conventional amplitude slice) for seismic data produced using raw amplitude and RMS options. Note very strong amplitude anomaly in the southeastern part of the map, which could indicate shallow gas sand with high amplitude anomaly on the amplitude map. The channel feature is clearly shown in the red color key (3800 - 4698) around the wells.

been carried out on the seismic data of inline range (1489 - 1819) and x-line range (4992 - 5425) within 2000 - 2400 ms. The seismic data spectrally decomposed as 15 Hz (low frequency), 23 Hz, 31 Hz (mid frequency), 39 Hz and 46 Hz (high frequency).

Amplitude variations were found to be around the potential gas reservoir. It can be investigated that the time frequency slice of 15 Hz, 23 Hz provide clearer event (potential hydrocarbon sand) indicated by high amplitude envelope (1172 - 1550) and amplitude anomalies around the potential gas reservoir. However, the high amplitude remains relative constant at (15 Hz) and (23 Hz) but the amplitude drops dramatically in the mid frequency (31 Hz), with some spots of high amplitude envelope but the high energy completely disappeared in 39 Hz time frequency slice. This can be interpreted as an attenuation artefact useful for hydrocarbon detection (**Figure 10**).

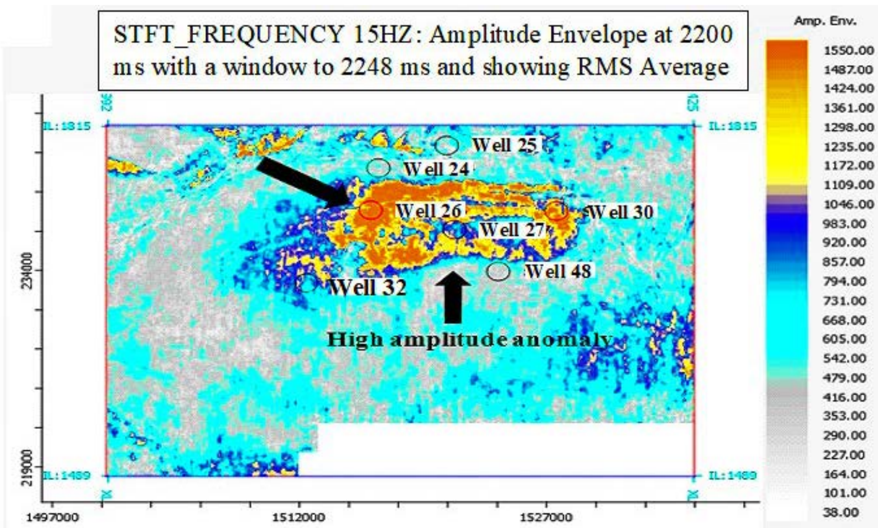

(a)

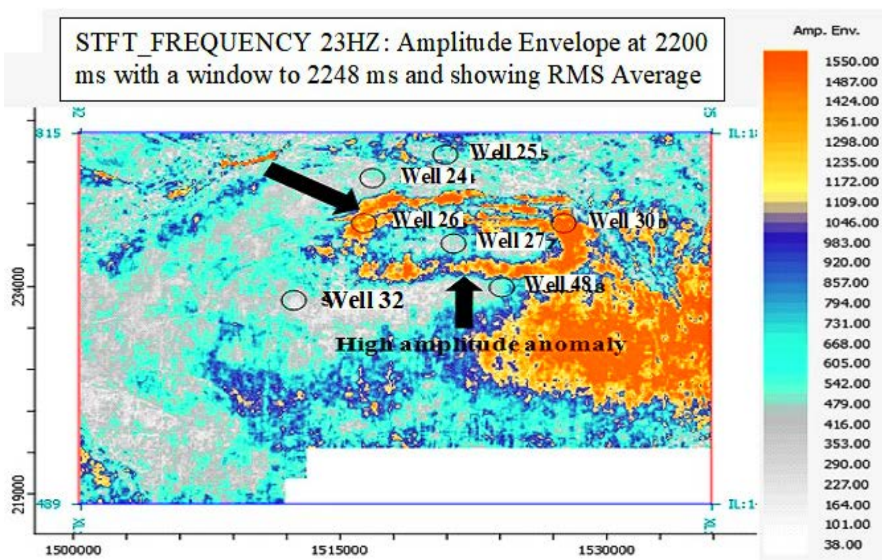

(b)

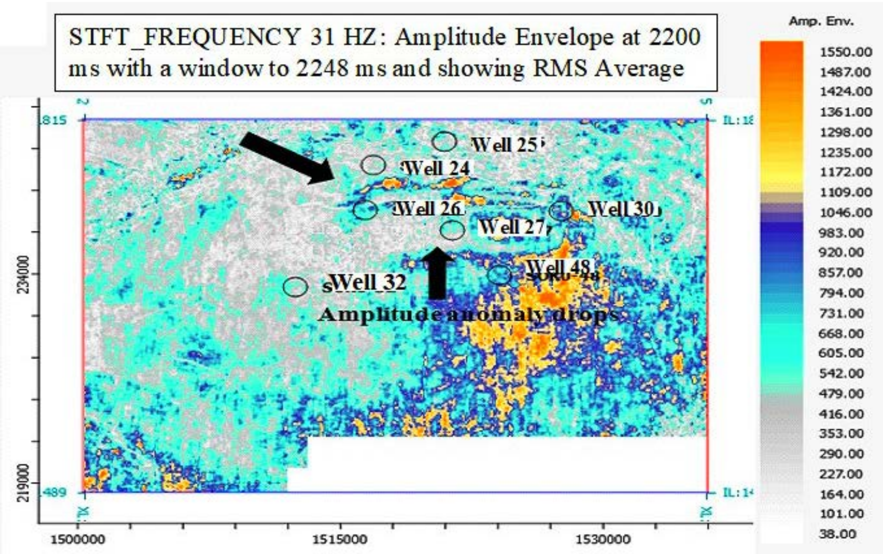

(c)

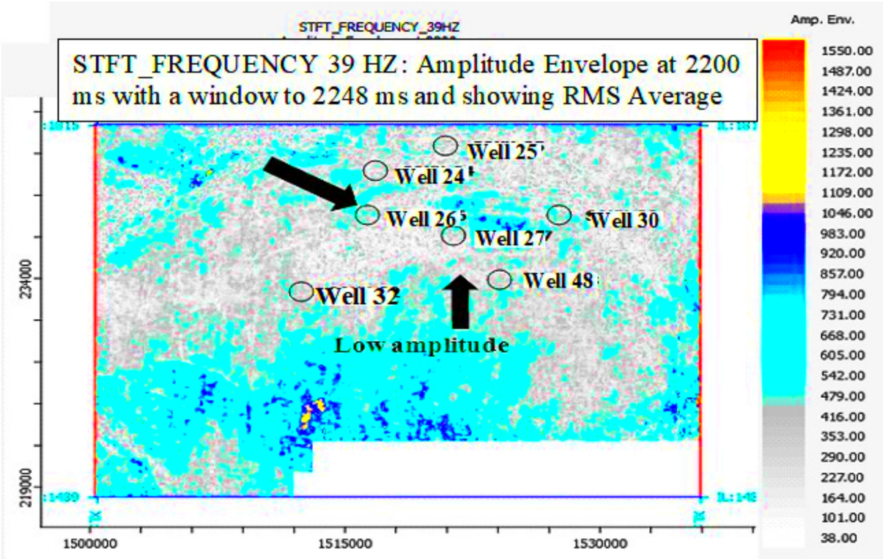

(d)

Figure 10. (a) Time frequency (15 Hz) section (amplitude slice) produced using amplitude envelope and RMS option from short time Fourier transform algorithm. (b) Time frequency (23 Hz) section (amplitude slice) produced using amplitude envelope and RMS option from short time Fourier transform algorithm. (c) Time frequency (31 Hz) section (amplitude slice) produced using amplitude envelope and RMS option from short time Fourier transform algorithm. (d) Time frequency (39 Hz) section (amplitude slice) produced using amplitude envelope and RMS option from short time Fourier transform algorithm.

4.2. Basic Pursuit

Also in this analysis, the seismic data was decompose using five frequencies, that is, 15 Hz (low frequency), 23 Hz, 31 Hz (mid frequency), 39 Hz and 46 Hz (High frequency) to assess the response of the potential reservoir or target zone. The Basic Pursuit algorithm has been applied on the seismic data of inline range (1489 - 1819) and x-line range (4992 - 5425) within 2000 - 2400 ms.

Amplitude variations were found around the potential gas reservoir place. Figures 11(a)-(d) show the time frequency section for the frequencies of 15 Hz (Figure 11(a)), 23 Hz (Figure 11(b)), 31 Hz (Figure 11(c)), 39 Hz (Figure 11(d)) and 46 Hz (Figure 11(e)). it can be investigated that the time frequency slice of 15 Hz, 23 Hz and 31 Hz provide clearer event (potential hydrocarbon sand) indicated by high amplitude envelope (1172 - 1550) and amplitude anomalies around the potential gas reservoir as indicated by black arrows. The high amplitude remains relative constant at (15 Hz), (23 Hz) and (31 Hz) but drops dramatically in the high frequency (39 Hz and 46 Hz), Figure 11(d) and Figure 11(e) with some spots of high amplitude envelope. This can be interpreted as an attenuation artefact useful for hydrocarbon detection.

4.3. Comparison between Short-Time Fourier Transform and Basic Pursuit Algorithm

The comparison of the two Algorithms of the produced sections of the time frequencies is shown in Figure 12(a) and Figure 13(a) (short-time Fourier transform) and Figure 12(b) and Figure 13(b) (Basic Pursuit technique). It was observed that the Basic Pursuit algorithm produced better frequency resolution compared to the Short-time Fourier transforms, particularly in the target zone between the two horizons. The potential gas sand event is indicated in the Basic Pursuit Algorithm at 31 Hz time frequency slice whereas in the short time, Fourier transform, the potential gas sand anomaly drops dramatically only showing some pockets of high energy in the 31 Hz time frequency slice respectively (Figure 13(a) and Figure 13(b)). This indicates the shortcoming of the Short-Time Fourier Transform. Even though, these two methods indicate the same anomaly in the target zone especially in the 15 Hz (low frequency) and 23 Hz, however, the Basic Pursuit Algorithm shows a clear continuity and detailed event around the wells.

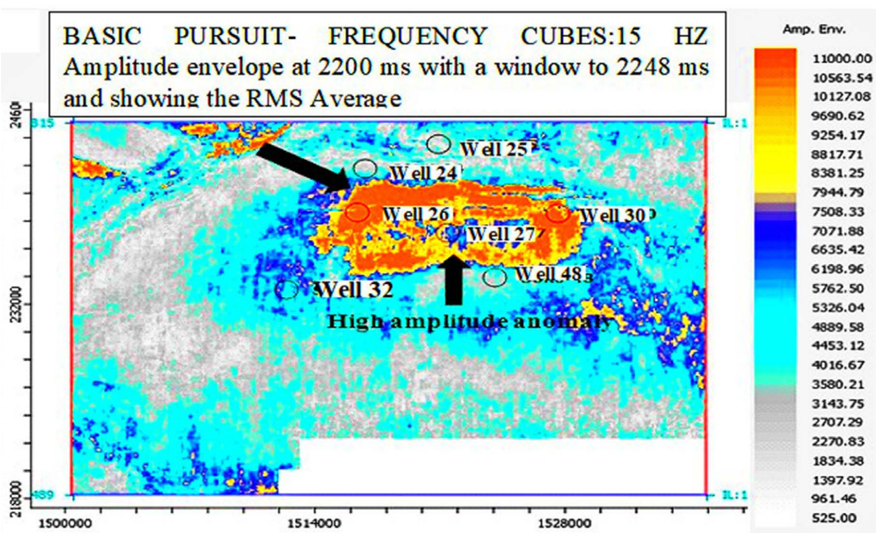

(a)

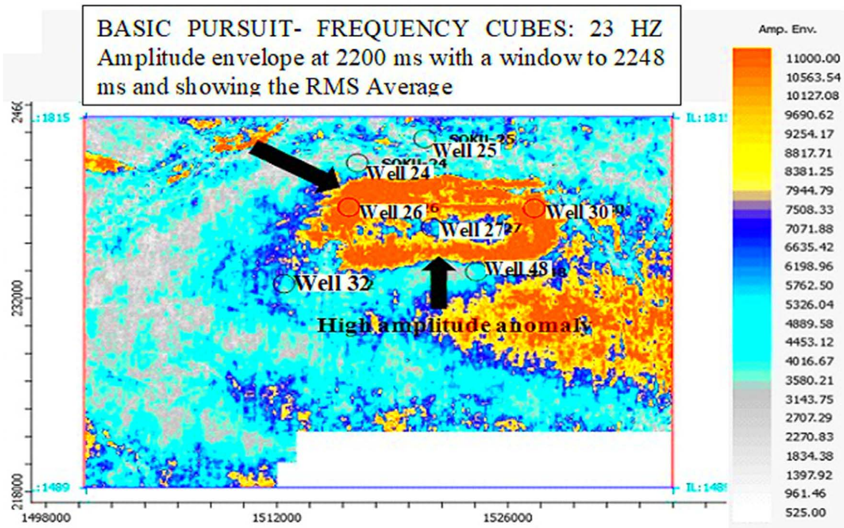
BASIC PURSUIT- FREQUENCY CUBES: 23 HZ
Amplitude envelope at 2200 ms with a window to 2248 ms and showing the RMS Average
Well 25
Well 24
Well 26
Well 30
Well 27
Well 48
Well 32
High amplitude anomaly
Amp. Env.
11000.00
10563.54
10127.08
9690.62
9254.17
8817.71
8381.25
7944.79
7508.33
7071.88
6635.42
6198.96
5762.50
5326.04
4889.58
4453.12
4016.67
3580.21
3143.75
2707.29
2270.83
1834.38
1397.92
961.46
525.00
1498000
1512000
1526000
232000
218000

(b)

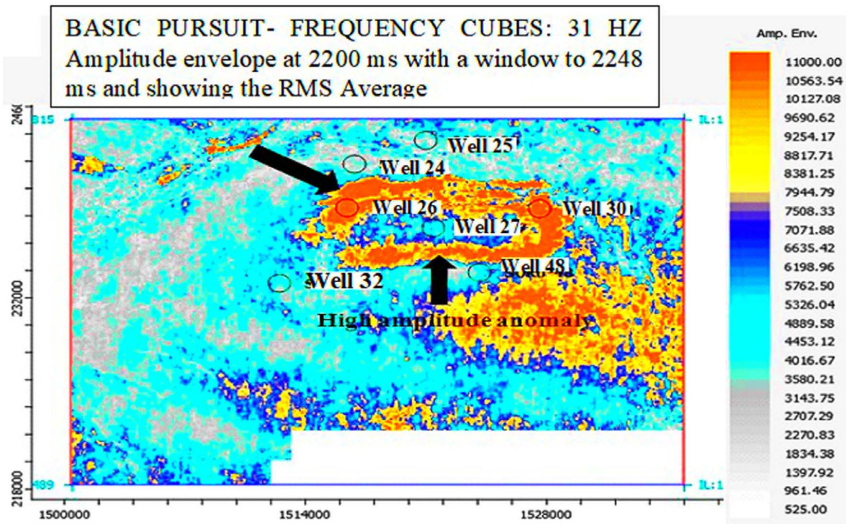
BASIC PURSUIT- FREQUENCY CUBES: 31 HZ
Amplitude envelope at 2200 ms with a window to 2248 ms and showing the RMS Average
Well 25
Well 24
Well 26
Well 30
Well 27
Well 48
Well 32
High amplitude anomaly
Amp. Env.
11000.00
10563.54
10127.08
9690.62
9254.17
8817.71
8381.25
7944.79
7508.33
7071.88
6635.42
6198.96
5762.50
5326.04
4889.58
4453.12
4016.67
3580.21
3143.75
2707.29
2270.83
1834.38
1397.92
961.46
525.00
1500000
1514000
1528000
232000
218000

(c)

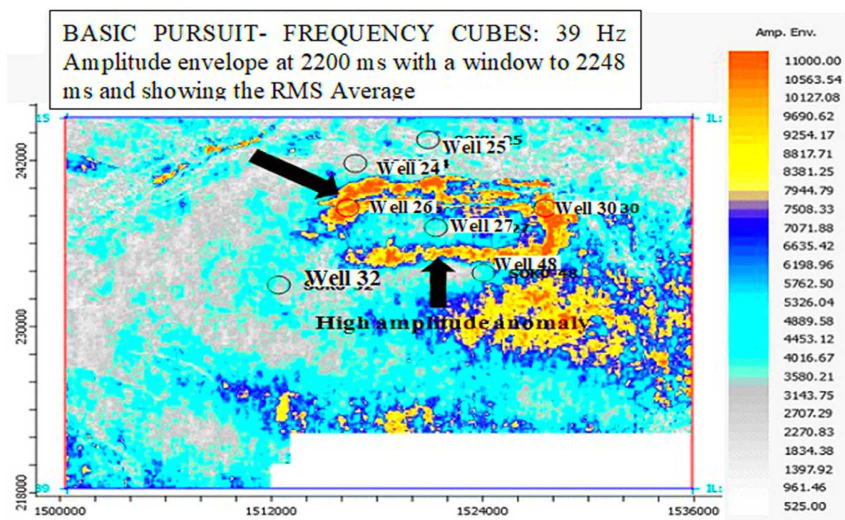
BASIC PURSUIT- FREQUENCY CUBES: 39 Hz
Amplitude envelope at 2200 ms with a window to 2248 ms and showing the RMS Average
Well 25
Well 24
Well 26
Well 30
Well 27
Well 48
Well 32
High amplitude anomaly
Amp. Env.
11000.00
10563.54
10127.08
9690.62
9254.17
8817.71
8381.25
7944.79
7508.33
7071.88
6635.42
6198.96
5762.50
5326.04
4889.58
4453.12
4016.67
3580.21
3143.75
2707.29
2270.83
1834.38
1397.92
961.46
525.00
1500000
1512000
1524000
1536000
242000
230000
218000

(d)

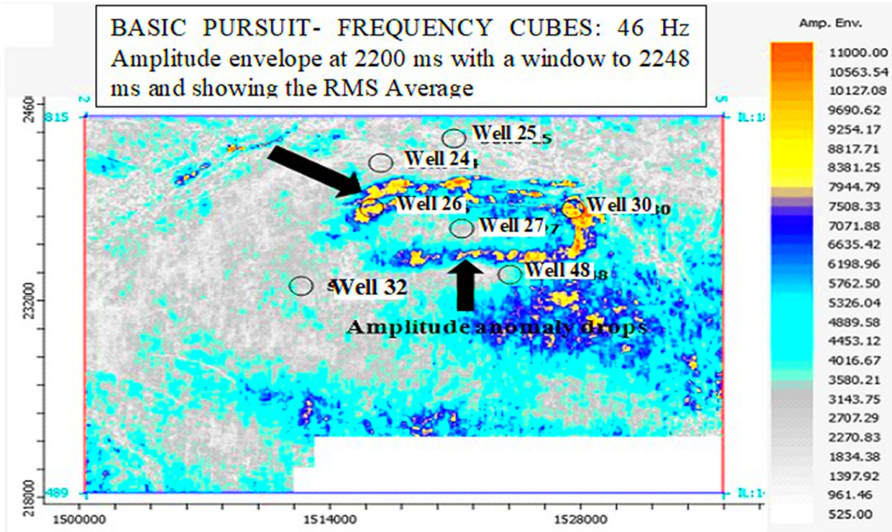

(e)

Figure 11. (a) Time frequency (15 Hz) section (amplitude slice) produced using amplitude envelope and RMS option from Basic Pursuit algorithm. (b) Time frequency (23 Hz) section (amplitude slice) produced using amplitude envelope and RMS option from Basic Pursuit algorithm. (c) Time frequency (31 Hz) section (amplitude slice) produced using amplitude envelope and RMS option from Basic Pursuit algorithm. (d) Time frequency (39 Hz) section (amplitude slice) produced using amplitude envelope and RMS option from Basic Pursuit algorithm. (e) Time frequency (46 Hz) section (amplitude slice) produced using amplitude envelope and RMS option from Basic Pursuit algorithm.

RGB COLOUR BLENDING OF THE FREQUENCY SLICES

In this section, the advanced 3D Visualization option was used to perform colour blending on these three volumes. Note that each of the frequency volumes defines the channel differently. A display of all three slices simultaneously will emphasize all of the subtle channel features. This involves inputting each of the frequency slices as a red, green or blue channel and mixing the colours. The black arrow indicates a pay reservoir. The three single-frequency sections shown in Figures 14(a)-(c) represent the 55 different frequencies computed between 5 to 60 Hz. It is clear to see that the channel responds to low frequency response when mixed. A set of models using the colour blending involving the Basic Pursuit algorithm was performed to validate the efficiency and consistency of the method in greater hydrocarbon identification in a reservoir. Of the frequency spectrum, the 15 hz was unique in better hydrocarbon identification. Three different colours RED, BLUE and GREEN were assigned to the 15 Hz interchangeably to generate models at different runs to evaluate its effectiveness in identifying the hydrocarbon saturated reservoir. The 3 runs were shown in Figures 14(a)-(c) where the 15 Hz was in turn assigned colours of RED, GREEN and BLUE respectively. For each run, a set of 3 frequencies 15 Hz, 23 Hz and 31 Hz were chosen and assigned these 3 colours. Figure 14(a) shows the colour blending with the following frequency/colour combination: 15 Hz/RED, 23 Hz/GREEN and 31 Hz/BLUE. The result show that for each run of the colour blending, the colour assigned to 15 Hz covered the part of the composite volume of the reservoir that was saturated by hydrocarbon. Hence, Figures 14(a)-(c) showed hydrocarbon saturation at 15 Hz/RED, 15 Hz/BLUE and 15 Hz/GREEN respectively. Note that for each clour blemding model, the rest of the other composite colour were assigned the other 2 sets of frequencies, 23 Hz and 51 Hz. The distribution of the colour blemds for each model is as shown in each Figures 14(a)-(c).

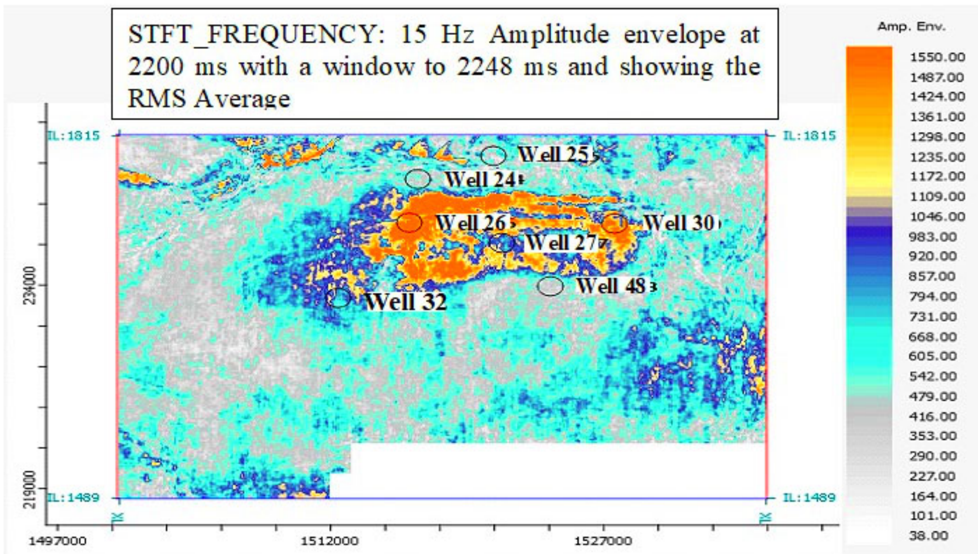

(a)

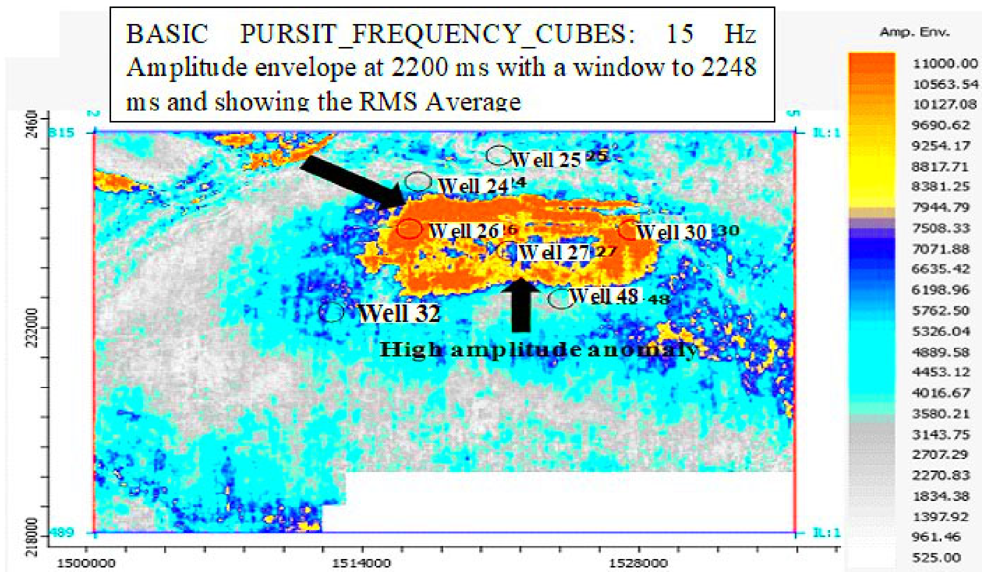

(b)

Figure 12. (a) Time frequency (15 Hz) section (amplitude slice) produced using amplitude envelope and RMS option from Short time Fourier transform algorithm. (b) Time frequency (15 Hz) section (amplitude slice) produced using amplitude envelope and RMS option from Basic Pursuit algorithm.

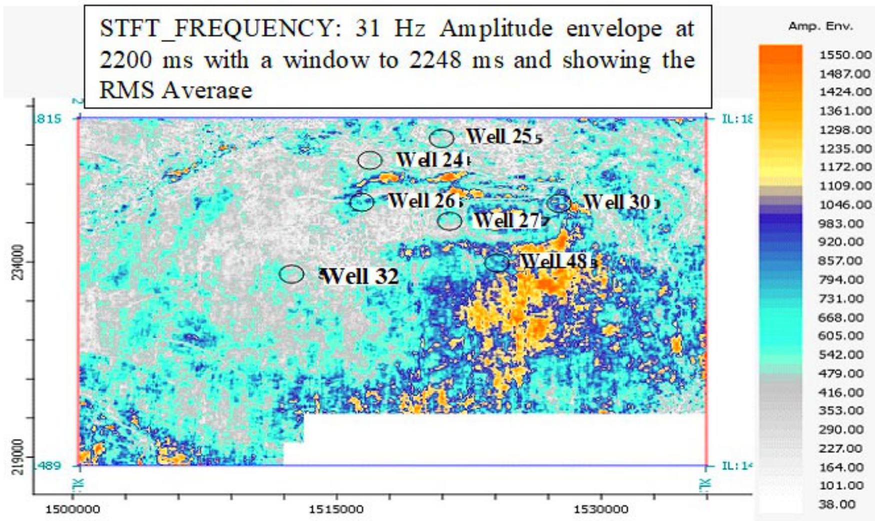

(a)

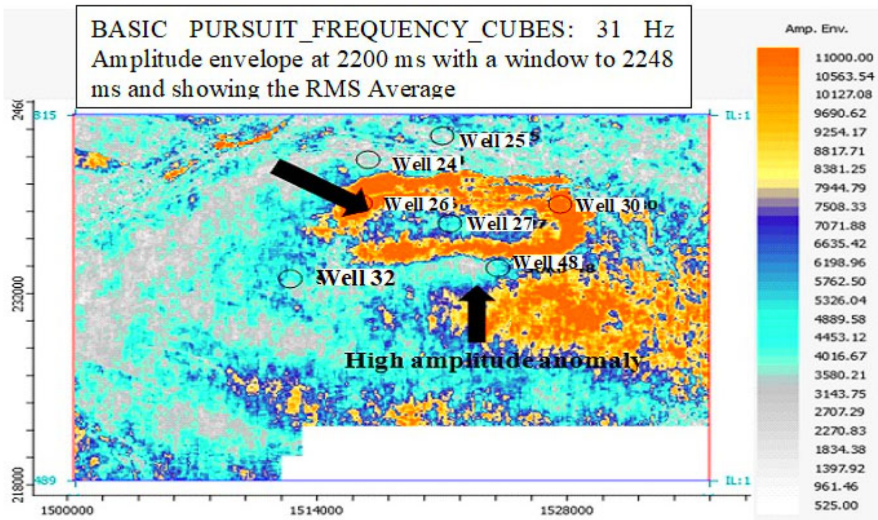

(b)

Figure 13. (a) Time frequency (31 Hz) section (amplitude slice) produced using amplitude envelope and RMS option from short time Fourier transform algorithm. (b) Time frequency (31 Hz) section (amplitude slice) produced using amplitude envelope and RMS option from Basic Pursuit algorithm.

The short-time Fourier transform and wavelet transform are well-known and well-proven time-frequency analysis tools. They both decompose the seismic signal with their pre-defined basis. Their main shortcomings are spectral smearing and the trade-off between time and frequency localization. Despite this, they remain popular because they produce smooth and robust features as shown in the above examples.

Our recommendation is to analyze the principal frequency variations by short-time Fourier transform or wavelet transform first, followed by identification of the subtle changes in geology using any advanced method like Basic Pursuit or CEEMD in a smaller time window.

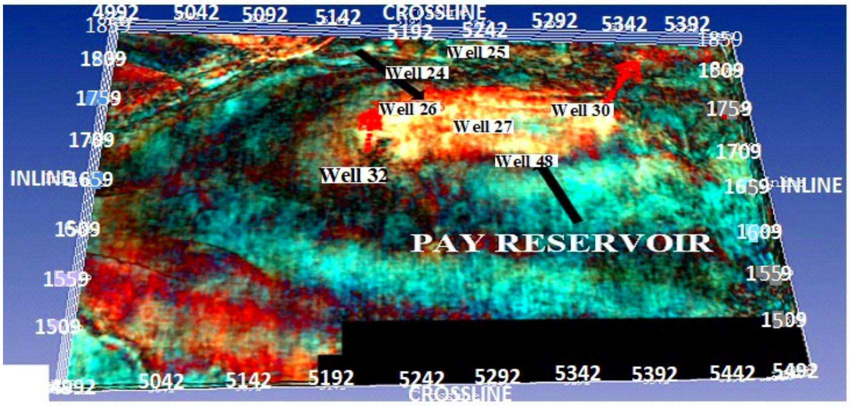

(a)

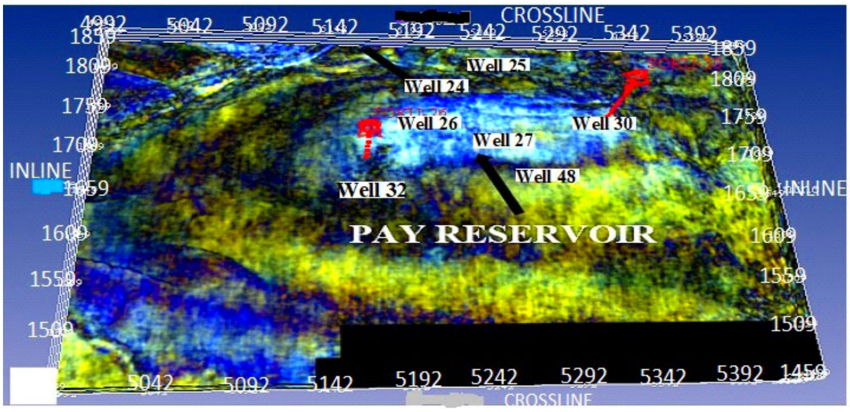

(b)

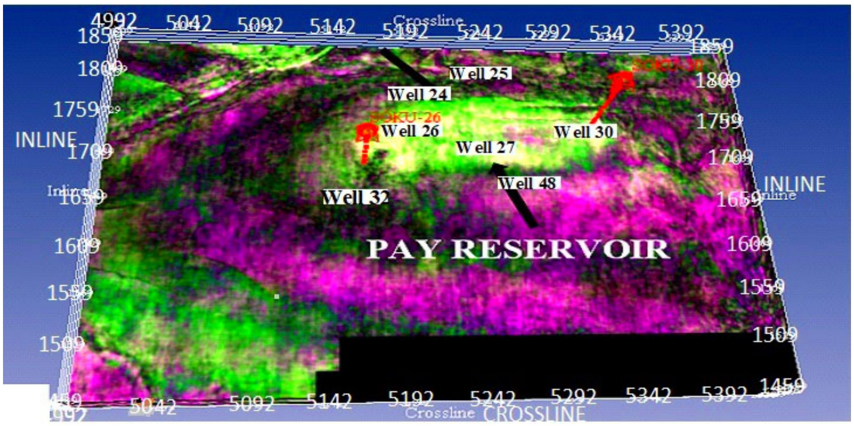

(c)

Figure 14. (a) Basic Pursuit algorithm time slice of composite volumes of constant frequency of RED = 15 Hz, GREEN = 23 Hz and BLUE = 31 Hz. The red channel is consistent with the low frequency section and the amplitude anomaly indicating potential hydrocarbon sand. (b) Basic Pursuit algorithm time slice of composite volumes of constant frequency of RED = 39 Hz, GREEN = 31 Hz and BLUE = 15 Hz. The blue channel is consistent with the low frequency section and the amplitude anomaly indicating potential hydrocarbon sand. (c) Basic Pursuit algorithm time slice of composite volumes of constant frequency of RED = 31 Hz, GREEN = 15 Hz and BLUE = 39 Hz. The green channel is consistent with the low frequency section and the amplitude anomaly indicating potential hydrocarbon sand.

There is no one "best" way to combine the volumes since each combination highlights different features.

5. Conclusion

Both the Fourier and Basic Pursuit Transform algorithms were employed in a Spectral decomposition method to successfully appraise their potential and efficiency in evaluating the hydrocarbon potential of the reservoir. The reservoir sand delineation revealed that the reservoir lies between TVD (ft) of 10,350 - 10,450 ft. The amplitude spectrum of the seismic data revealed that the frequency spectrum peaked between 5 Hz and 60 Hz. The high amplitude obtained in the low frequency (15 Hz - 25 Hz) band in the gas reservoir is a consistent character of the over-pressured gas reservoirs in the Niger Delta basin. The time-frequency slices of 15 Hz and 23 Hz provided clearer events representing potential hydrocarbon-saturated sand. This is indicated by the high amplitude envelope of 1172 - 1550 and the amplitude anomalies around the potential gas reservoir. However, the amplitude drops dramatically in the mid-frequency (31 Hz), high amplitude envelope and the high energy completely disappeared in the high frequency (46 Hz) time-frequency slice. This can be interpreted as an attenuation signature useful for hydrocarbon detection. A comparison of the Short-time Fourier transform and Basic Pursuit model revealed that Basic Pursuit gave a better resolution for this analysis than the former and thus is a recommended technique for spectral analysis application in hydrocarbon reservoir evaluation. The Red, Green and Blue colour blending model showed that the channel was consistent with the low-frequency section and the amplitude anomaly indicating potential hydrocarbon sand in that portion of the reservoir. Using AVO as a complementary technique to this analysis is recommended.

Acknowledgements

The authors wish to thank the Department of Petroleum Resources and SPDC Port Harcourt for the release of the data for this study.

Author Contribution

OSO conceptualized the study and collected the data. Both OSO and UCC undertook the project design, material preparation, analysis and interpretations. UCC supervised and edited the final version of this work and prepared it for submission.

Conflicts of Interest

The authors declare no conflicts of interest regarding the publication of this paper.

References

[1] Chakraborty, A. and Okaya, D. (1995) Frequency-Time Decomposition of Seismic

Data Using Wavelet-Based Methods. *Geophysics*, **60**, 1906-1916. https://doi.org/10.1190/1.1443922

[2] Sinha, S., Routh, P.S., Anno, P.D. and Castagna, J.P. (2005) Spectral Decomposition of Seismic Data with Continuous-Wavelet Transform. *Geophysics*, **70**, 19-25. https://doi.org/10.1190/1.2127113

[3] Stockwell, R.G., Mansinha, L. and Lowe, R.P. (1996) Localization of the Complex Spectrum: The S Transform. *IEEE Transactions on Signal Processing*, **44**, 998-1001. https://doi.org/10.1109/78.492555

[4] Liu, J.L. and Marfurt, K. (2007) Multi-Color Display of Spectral Attributes. *The Leading Edge*, **26**, 268-271. https://doi.org/10.1190/1.2715047

[5] Bacon, M., Simm, R. and Redshaw, T. (2007) 3-D Seismic Interpretation. Cambridge University Press, Cambridge, 224.

[6] Hermana, M., Ghosh, D.P. and Sum, C.W. (2016) Optimizing the Lithology and Pore Fluid Separation Using Attenuation Attributes. *The Offshore Technology Conference Asia*, Kuala Lumpur, March 2016, OTC-26437-MS. https://doi.org/10.4043/26437-MS

[7] Brown, A.R. (2001) Understanding Seismic Attributes. *Geophysics*, **66**, 47-48. https://doi.org/10.1190/1.1444919

[8] Partyka, G., Gridley, J. and Lopez, J.A. (1999) Interpretational Applications of Spectral Decomposition in Reservoir Characterization. *The Leading Edge*, **18**, 353-360. https://doi.org/10.1190/1.1438295

[9] Miao, X. and Cheadle, S. (1998) High Resolution Seismic Data Analysis by Wavelet Transform and Matching Pursuit Decomposition: Modeling Study. *Geophysics*, **59**, 1849-1855.

[10] Chapman, M., Liu, E. and Li, X.Y. (2005) The Influence of Abnormally High Reservoir Attenuation on the AVO Signature. *The Leading Edge*, **24**, 1120-1125. https://doi.org/10.1190/1.2135103

[11] Chapman, M., Liu, E. and Li, X.Y. (2006) The Influence of Fluid Sensitive Dispersion and Attenuation on AVO Analysis. *Geophysical Journal International*, **167**, 89-105. https://doi.org/10.1111/j.1365-246X.2006.02919.x

[12] Odebeatu, C.O., Zhang, J., Chapman, M., Liu, E. and Li, X.-Y. (2006) Application of Spectral Decomposition to Detection of Dispersion Anomalies Associated with Gas Saturation. *The Leading Edge*, **25**, 206-210. https://doi.org/10.1190/1.2172314

[13] Zhang, H. and Brown, R.J. (2001) A Review of AVO Analysis. CREWES Research Report 13.

[14] Young, K.T. and Tatham, R.H. (2007) Fluid Discrimination of Poststack "Bright Spots" in the Columbus Basin, Offshore Trinidad. *The Leading Edge*, **26**, 1508-1515. https://doi.org/10.1190/1.2821936

[15] Peel, F.J. and White, J. (2016) Do Technical Studies Reduce Subsurface Risk in Hydrocarbon Exploration: And If Not, How Do They Add Value? *Geological Society, London, Special Publications*, **436**, 247-259. https://doi.org/10.1144/SP436.4

[16] Obiekezie T.N. and Bassey, E.E. (2015) 3D Structural Analysis of Otu Field, Niger Delta, Nigeria. *Physical Science International Journal*, **7**, 114-126. https://doi.org/10.9734/PSIJ/2015/16512

[17] Asubiojo, T.M. and Okunuwadje, S.E. (2016) Petrophysical Evaluation of Reservoir Sand Bodies in Kwe Field Onshore Eastern Niger Delta. *Journal of Applied Sciences and Environmental Management*, **20**, 383-393. https://doi.org/10.4314/jasem.v20i2.21

[18] Emina, R., Obiadi, I.I. and Obiadi, C.M. (2016) Evaluation and Prospect Identification in the Olive Field, Niger Delta Basin, Nigeria. *Journal of Petroleum & Environmental Biotechnology*, **7**, Article ID: 1000284. https://doi.org/10.4172/2157-7463.1000284

[19] Olawale, O.O., Ajayi, F.S. and Akeye, N.A. (2017) Evaluation of Petrophysical Properties for Reservoir Characterization of AK Field, Onshore Eastern Niger Delta, Southern Nigeria. *Journal of Mining and Geology*, **53**, 67-77.

[20] Farfour, M., Ferahtia, J., Djarfour, N. and Aitouch, M.A. (2018) Seismic Spectral Decomposition Applications in Seismic: A Review and Application. In: Gaci, S. and Hachay, O., Eds., *Oil and Gas Exploration*: *Methods and Application*, American Geophysical Union, Washington DC, 93-113. https://doi.org/10.1002/9781119227519.ch6

[21] Castagna, J.P., Sun, S. and Siegfried, R.W. (2003) Instantaneous Spectral Analysis: Detection of Low-Frequency Shadows Associated with Hydrocarbons. *The Leading Edge*, **22**, 120-127. https://doi.org/10.1190/1.1559038

[22] Peyton, L., Bottjer, R. and Partyka, G. (1998) Interpretation of Incised Valleys Using New 3-D Seismic Techniques: A Case History Using Spectral Decomposition and Coherency. *The Leading Edge*, **17**, 1294-1298. https://doi.org/10.1190/1.1438127

[23] Hardy, H.H., Beier, R.A. and Gaston, J.D. (2003) Frequency Estimates of Seismic Traces. *Geophysics*, **68**, 370-380. https://doi.org/10.1190/1.1543222

[24] Kulke, H. (1995) Regional Petroleum Geology of the World. Part II: Africa, America, Australia and Antarctica. Gebruder Borntraeger, Berlin, 143-172.

[25] Roberts, D.G. and Bally, A.W. (2012) Regional Geology and Tectonics: Phanerozoic Passive Margins, Cratonic Basins and Global Tectonic Maps. Vol. 1, Elsevier, Amsterdam, 1196. https://doi.org/10.1016/B978-0-444-56357-6.00025-1

[26] Onojake, M.C., Osuji, L.C. and Abrakasa, S. (2015) Source, Depositional Environment and Maturity Levels of Some Crude Oils in Southwest Niger Delta, Nigeria. *Chinese Journal of Geochemistry*, **34**, 224-232. https://doi.org/10.1007/s11631-015-0035-9

[27] Oyedele, K.F., Ogagarue, D.O. and Mohammed, D.U. (2013) Integration of 3D Seismic and Well Log Data in the Optimal Reservoir Characterisation of Emi Field, Offshore Niger Delta Oil Province, Nigeria. *American Journal of Scientific and Industrial Research*, **4**, 11-21. https://doi.org/10.5251/ajsir.2013.4.1.11.21

[28] Liu, J.-P., *et al*. (2008) Petroleum Geology and Resources in West Africa: An Overview. *Petroleum Exploration and Development*, **35**, 378-384. https://doi.org/10.1016/S1876-3804(08)60086-5

[29] Moshood, O.A. and Bamford, K.M. (2019) Depositional Environment and Reservoir Characterization of the Deep Offshore Upper Miocene to Early Pliocene Agbada Formation, Niger Delta, Nigeria. *Journal of African Earth Sciences*, **159**, Article ID: 103578. https://doi.org/10.1016/j.jafrearsci.2019.103578

[30] Edigbue, P.I., Komolafe, A.A., Adesida, A.A. and Itamuko, O.J. (2014) Hydrocarbon Reservoir Characterization of "Keke" Field, Niger Delta Using 3D Seismic and Petrophysical Data. *Standard Global Journal of Geology and Explorational Research*, **2**, 43-52.

[31] Selley, R.C. (2004) Petroleum Geology of Africa: New Themes and Developing Technologies. *Geological Magazine*, **141**, 749-750.

[32] Aturamu Adeyinka, O., Ojo Adebayo, O., Adebayo Olajide, F. and Akinyemi Segun, A. (2015) Palynostratigraphic Analysis of the Agbada Formation (Nep-1 Well) Offshore, Eastern Niger-Delta Basin, Nigeria. *British Journal of Environmental Sciences*,

3, 19-31.

[33] Iheanyichu, O.A. and Jac, O.L. (2018) 3-D Seismic Attribute Analysis for Enhanced Prospect Definition of “Opu Field”, Coastal Swamp Depobelt Niger Delta, Nigeria. *Journal of Applied Sciences*, **18**, 86-102. https://doi.org/10.3923/jas.2018.86.102

[34] Nwajide, C.S. (2013) Geology of Nigeria’s Sedimentary Basins. CSS Bookshops Ltd., Lagos, 565.

[35] Chen, G., Matteucci, G., Fahmy, B. and Finn, C. (2008) Spectral-Decomposition Response to Reservoir Fluids from a Deepwater West Africa Reservoir. *Geophysics*, **73**, C23-C30. https://doi.org/10.1190/1.2978337